Published in final edited form as:
Dev Dyn. 2009 October ; 238(10): 2550–2563. doi:10.1002/dvdy.22086.

Craniofacial skeletal defects of adult zebrafish *glypican 4 (knypek)* mutants

Elizabeth E. LeClair[1], **Stephanie R. Mui**[2], **Angela Huang**[1], **Jolanta M. Topczewska**[2], and **Jacek Topczewski**[2,3]

[1] Department of Biological Sciences, DePaul University, 2325 N. Clifton Ave. Chicago, IL 60614

[2] Children's Memorial Research Center and Department of Pediatrics, Northwestern University Feinberg School of Medicine, 2300 Children's Plaza Box 204, Chicago, IL 60614

Abstract

The heparan sulfate proteoglycan Glypican 4 (Gpc4) is part of the Wnt/planar cell polarity pathway, which is required for convergence and extension during zebrafish gastrulation. To observe Glypican 4-deficient phenotypes at later stages, we rescued *gpc4*$^{-/-}$ (*knypek*) homozygotes and raised them for more than one year. Adult mutants showed diverse cranial malformations of both dermal and endochondral bones, ranging from shortening of the rostral-most skull to loss of the symplectic. Additionally, the adult palatoquadrate cartilage was disorganized, with abnormal chondrocyte orientation. To understand how the palatoquadrate cartilage normally develops, we examined a juvenile series of wild type and mutant specimens. This identified two novel domains of elongated chondrocytes in the larval palatoquadrate, which normally form prior to endochondral ossification. In contrast, *gpc4*$^{-/-}$ larvae never form these domains, suggesting a failure of chondrocyte orientation, though not differentiation. Our findings implicate Gpc4 in the regulation of zebrafish cartilage and bone morphogenesis.

Keywords (10)

zebrafish; glypican; *knypek*; craniofacial; skull; jaw; bone; cartilage; morphometrics

Introduction

Recent progress in developmental biology has shown that a few molecular signaling pathways control nearly all cell fates in an embryo (Barolo and Posakony, 2002). Mutations affecting these pathways can cause early, extreme phenotypic defects, rapidly identifying key developmental genes. Much less is known, however, about how the same signaling pathways are redeployed later in ontogeny, affecting tissue maturation and growth. Within the zebrafish system, for example, embryonic mutagenesis screens have generated hundreds of developmentally altered embryos (Neuhauss et al., 1996; Piotrowski et al., 1996; Geisler et al., 2007) review by (Amsterdam and Hopkins, 2006), but fewer have been followed to the juvenile or adult stages (Fisher et al., 2003; Elizondo et al., 2005; Gavaia et al., 2006; Albertson and Yelick, 2007). In this report, we examine the consequences of mutations in the *knypek* gene, a zebrafish homolog of mammalian *glypican 4*. The glypican (GPC) family of extracellular proteins regulates key developmental processes by modulating the signaling of Wnts, Bmps and Fgfs among other ligands (Filmus and Selleck, 2001; Fransson, 2003). Once secreted, glypicans have their C-termini anchored to the cell membrane by

[3]Corresponding author: J-Topczewski@northwestern.edu, phone 773 755 6545, fax 773 755 6385.

glycosylphosphatidylinositol, and thus lack a cytoplasmic domain. The extracellular core protein is modified by multiple heparan sulfate side chains that are thought to capture diffusible ligands, regulating their presentation to cell surface receptors. Glypicans are thus well placed to act as extracellular 'gatekeepers,' regulating various signaling pathways.

Glypicans are conserved in both invertebrates and vertebrates (Filmus and Selleck, 2001). There are two *Drosophila* genes, *dally* and *dally-like* (Nakato et al., 1995; Khare and Baumgartner, 2000), and one *Caenorhabditis* gene, *lon-2* (Gumienny et al., 2007). In mammals, six glypicans (GPC1-GPC6) have been identified. Mutation of the human *GPC3* gene has been linked to Simpson-Golabi-Behmel Syndrome (Pilia et al., 1996), which causes congenital heart defects, dysplastic kidneys, embryonal tumors, and various skeletal defects. *Gpc3* deficient mice show a similar spectrum of developmental problems (Cano-Gauci et al., 1999; Paine-Saunders et al., 2000; Chiao et al., 2002), including delayed endochondral ossification due to reduced osteoclast function (Viviano et al., 2005). The developmental roles of other human glypicans, however, are not fully understood.

In zebrafish, positional cloning identified that *knypek* (*kny*) is homologous to human *glypican 4* (*gpc4*) (Solnica-Krezel et al., 1996; Topczewski et al., 2001). *Gpc4* is to date the best-studied zebrafish glypican, and several alleles have been isolated. The amorphic allele kny^{fr6} contains a premature stop codon (S247) in the middle of the core protein, causing a complete loss of function. In contrast, the hypomorphic allele kny^{m818} has a single missense substitution (Q527P) near the GPI attachment site (Topczewski et al., 2001). *gpc4* is maternally expressed and remains uniformly distributed in zebrafish blastomeres from fertilization through 30% epiboly. At gastrulation, *gpc4* is concentrated at the dorsal blastoderm margin, and remains strongly expressed in dorso-lateral tissues form the late gastrula stage through somitogenesis. Proper expression at these stages is essential for normal development, as $gpc4^{-/-}$ embryos have severely reduced convergence and extension movements in both ectodermal and mesendodermal cell populations (Topczewski et al., 2001). Mutant cells are unable to undergo effective mediolateral elongation and intercalation, leading to broader and shorter embryos that do not survive past 5–7 days post fertilization. Moreover, *glypican 4* is expressed after gastrulation in different tissues, including regions of the head where the neurocranium and pharyngeal cartilage elements are formed (Topczewski *et al.* 2001; Supplementary Figure S1).

We have previously demonstrated that injections of *gpc4* mRNA into fertilized $gpc4^{-/-}$mutant eggs can rescue gastrulation movements with high efficiency (Topczewski et al., 2001). Although the injected larvae have normal axial lengths, not all aspects of the mutant phenotype are equally restored. Specifically, at 5 dpf the rescued larvae still display a "hammerhead" appearance, lacking the bulb of tissue normally protruding rostral to the eyes. At the cellular level, the larval cranial cartilages are shortened, and the chondrocyte arrangement of these elements is disorganized. These results, in combination with the known expression of *gpc4* in the pharyngeal arches, suggested to us that in addition to an essential role in gastrulation movements, *gpc4* might contribute to craniofacial morphogenesis by regulating chondrocyte behavior and orientation.

The lethality of *gpc4* loss of function mutations demonstrates that this protein is essential for normal larval development, but makes it impossible to study whether *gpc4* is also required for later zebrafish development. In contrast to an extensive body of literature on early craniofacial development (3–7 dpf), only a few studies have described phenotypes in the adult zebrafish skull (Fisher and Halpern, 1999; Witten et al., 2001; Albertson and Yelick, 2004; Hunter and Prince, 2002). Although not as viable as their wild type siblings, rescued kny^{m818} homozygote fish can be reared to adult size (2–3 cm). By following these fish to maturity, we sought to discover developmental processes that were dependent on Glypican

4. In addition, we wanted to correlate the early defects in the larval head skeleton with the adult craniofacial phenotype.

We have found that rescued *gpc4*$^{-/-}$ adults display a characteristic craniofacial "syndrome", having smaller crania than wild type fish and a repeatable, highly penetrant set of bony defects. This was confirmed by a quantitative morphometric analysis of neurocranial shape and a qualitative comparison of other skull bones. Defective cartilage morphogenesis in *gpc4*$^{-/-}$larvae leads to the frequent absence of a specific bone, the symplectic, from the adult jaw suspensorium. Chondrocytes of the larval symplectic are unable to extend into a normal cartilage rod and fail to ossify. In the absence of symplectic ossification, adjacent skeletal structures develop abnormally, yet produce a jaw that retains some function. In addition to these bony defects, *gpc4*$^{-/-}$ zebrafish have disorganized chondrocyte arrangements in the adult palatoquadrate cartilage, a connective element of the kinetic teleost skull. Normally, chondrocytes within this element arrange into two highly elongated arcs at the onset of endochondral ossification. In *gpc4*$^{-/-}$ larvae, these chondrocytes are disorganized, suggesting a loss of polarity; in the adult, the mutant cartilage forms an abnormal connection to adjacent bones. These late-stage cartilage defects in *gpc4*$^{-/-}$ mutants suggest an ongoing ontogenetic role for Glypican 4 in regulating cartilage cell polarity, chondrocyte stacking and endochondral ossification, with complex consequences for the integrated process of fish skull development.

Results

gpc4$^{-/-}$ larvae retain disorganized craniofacial cartilages despite suppression of gastrulation defects by *gpc4* mRNA injection

The starting point for our investigation was the observation that *glypican 4* mRNA could rescue *gpc4*$^{-/-}$ mutant embryos from abnormal convergence and extension movements, but did not produce a completely normal phenotype. Although body length was restored (Topczewski et al., 2001), pharyngeal cartilage elements such as the palatoquadrate (Fig. 1A–D), symplectic (Fig. 1I–K), and ceratohyal (Fig. 1L–M) were shorter and thicker than normal. The anterior part of the ethmoid plate was shortened, and the hypophyseal fenestra was enlarged (Fig. 1E–H). In contrast, the more posteriorly located parachordal plate of the neurocranium was not affected. Injecting *gpc4* mRNA into wild type siblings of the mutants had no effect on the size or organization of any neurocranial cartilages (Fig. 1C, G).

Within each affected cartilage element, *gpc4*$^{-/-}$ chondrocytes appeared rounded and had abnormal stacking patterns. This stacking defect was especially severe in the larval symplectic. This single cartilage element eventually ossifies to become two adult bones; the flattened dorsal region becomes the hyomandibula, while the rod-shaped ventral region becomes the symplectic (Fig. 1I). In uninjected *gpc4*$^{-/-}$ larvae, the hyomandibular chondrocytes appeared relatively normal, but the symplectic chondrocytes failed to intercalate (Fig. 1J). Instead of forming a cartilage rod extending anteriorly, these cells remained bunched together, accumulating near the interhyal joint. The same phenotype was observed in *gpc4*$^{-/-}$ larvae receiving mRNA injections of *gpc4* (Fig. 1K). Because both injected and uninjected mutants showed the same cranial cartilage defects, this suggested that larval chondrocytes require Glypican 4 function for proper morphogenesis, a process not rescued by *gpc4* mRNA injected at the 1–2 cell stage.

One explanation for the shorter symplectic in *gpc4*$^{-/-}$ larvae would be that the number of cartilage cells is reduced, either by increased cell death or failure to proliferate. This was tested by counting the number of symplectic chondrocytes in 4 wild type and 5 *gpc4*$^{-/-}$ larvae, respectively. At 5 days post fertilization, there was no significant difference in cell number between the two groups (wild type, 50 cells +/− 5; *gpc4*$^{-/-}$, 50 cells +/− 5). Thus

differences in cell proliferation or death are unlikely the primary reason for the shortening of these cartilage elements.

Homozygous *gpc4*$^{-/-}$ adults have neurocranial defects

A small proportion of rescued *gpc4*$^{-/-}$ larvae survived to adulthood, allowing us to investigate how the loss of Gpc4 affects the mature craniofacial skeleton. In particular, we wished to know if the defective cartilages observed at the larval stages (*e.g*., Fig. 1) would have a lasting effect on the corresponding bones of mutant adults. Alternatively, we considered that post-larval growth – including cartilage replacement, dermal bone formation, and bone remodeling – might compensate for the early skeletal defects. We compared adult *gpc4*$^{-/-}$ fish (n=12) to comparably aged wild type fish (n=12) using whole-mount skeletal staining. All fish were >1 year in age and between 2.2 and 3.7 cm in standard length (SL, +/− 0.5 mm). The mutants and wild types were similar in post-cranial proportions, fin morphology, and branchial arch structures (data not shown). However, the mutants had disproportionately small heads, domed skulls, and short jaws. The severity of these phenotypes varied; a moderately affected *gpc4*$^{-/-}$ adult is shown (Fig. 2).

To quantify adult craniofacial variations both within and between groups, we digitized 20 neurocranial landmarks in left lateral view (Fig. 3A) and 33 neurocranial landmarks in ventral view (Fig. 3B) from the skulls of wild type and *gpc4*$^{-/-}$ specimens. Considered from either perspective, *gpc4*$^{-/-}$ neurocrania were significantly smaller than wild type neurocrania when compared using centroid size, a shape-independent measure of area (data not shown; one-tailed Mann-Whitney U test, $p<0.005$ for both tests). We next considered whether the smaller head size in mutants could be explained by smaller body sizes in this population, as was the case for our limited sample. However, bivariate regressions of skull centroid size *vs.* standard length (a proxy for “body size” in fishes) gave similar slopes, but highly different intercepts, for the two populations (Fig. 3C, D; $p < .0001$ for both tests). Thus *gpc4*$^{-/-}$ mutants have significantly smaller neurocrania relative to wild type fish across a wide range of adult body sizes, suggesting that the larval cranial defects are not rescued by postlarval growth.

When the size differences between wild type and *gpc4*$^{-/-}$ neurocrania were removed by Procrustes superimposition of the corresponding landmark configurations, the residual shape differences were also highly significant (Table 1). Relative to wild types, *gpc4*$^{-/-}$ neurocrania in lateral view had landmarks of the anterior ethmoid region (kinethmoid and lateral ethmoid bones) shifted posteriorly, and landmarks on the midskull (orbitosphenoid and parasphenoid bones) shifted anteriorly, indicating shorter bones in this region (Fig. 3E). The posterior neurocranium was much less altered, reflecting nearly the same shape for both groups. In ventral view, a similar pattern was observed (Fig. 3F). Landmarks of the anteriormost cranial bones were shifted posteriorly, indicating shortening of the intervening areas (kinethmoid, lateral ethmoid, orbitosphenoid, and parasphenoid bones), whereas mid-cranial and posterior landmarks were less affected. Taken together, our size and shape analyses indicate that *gpc4*$^{-/-}$ zebrafish, although individually variable, show a highly repeatable, statistically robust phenotype of anterior skull reductions that persist from larva to adult.

Loss of *glypican 4* function leads to loss of adult craniofacial bones

Following the quantitative analysis of the adult neurocranium, we next performed a qualitative analysis of the lateral facial bones, including the jaws and jaw suspensorium (Fig. 4A, B). *gpc4*$^{-/-}$ adults showed significant reshaping of both bone and cartilage elements, particularly in the region of the symplectic. Whereas all of the wild type fish had a normal, bilateral symplectics (12/12), 83% of the mutants showed either unilateral (4/12; Fig 4C, D)

or bilateral (6/12, Fig. 4E, F) loss of this element. Only two out of twelve adult *gpc4*$^{-/-}$ fish had both symplectics present. The failure of this bone to form strongly correlates with the observed larval phenotype in which the symplectic cartilage is composed of abnormally arranged chondrocytes that fail to extend (Fig. 1I–K).

In the absence of the adult symplectic, the adjacent metapterygoid was expanded ventrally, covering the entire dorsal margin of the quadrate (Fig. 4D–F). At this margin the metapterygoid and quadrate were connected by a deeply staining band of cartilage, a stub of which protruded into the depression on the quadrate where the symplectic bone usually lies. While in wild type fish the symplectic and metapterygoid were both attached to the more posterior hyomandibular (not shown), in *gpc4*$^{-/-}$ adults only the metapterygoid occupied this position. These rearrangements of the facial bones and cartilages surrounding the symplectic were observed consistently in the population of mutants, indicating a repeated developmental response that allowed some adults to survive with an altered, yet functional, set of jaw linkages.

Intermediate stages of symplectic development in *gpc4*$^{-/-}$ juveniles

To investigate how the symplectic bone was lost from *gpc4*$^{-/-}$ adults, we returned to examine some intermediate stages of chondrogenesis and osteogenesis in mutant juveniles. To do this, we performed additional rescue experiments on both *kny*^{m818} and *kny*^{fr6} embryos. Eggs from a cross of heterozygote parents were injected with *glypican 4* mRNA at the one-cell stage; a portion of each clutch was set aside to serve as a non-injection control. At 4–5 dpf, rescued *gpc4*$^{-/-}$ embryos could be recognized by their “hammerhead” appearance. To reduce competition between mutant and wild type siblings, the fish were sorted by phenotype into separate tanks and raised under identical conditions to the desired stage.

At 7–8 mm standard length (~2–3 weeks at 28.5°C), injected wild type larvae showed normal development of the lateral facial bones (Fig. 5A, C). The symplectic was a separate rod posterior and ventral to the metapterygoid bone. Endochondrial ossification of symplectic was already underway, leaving two cartilaginous ends. The anterior end of the symplectic rested on a bony spur of the quadrate bone that projected posteriorly. The posterior end of the symplectic was still partially fused to the hyoid and the small, cartilaginous interhyal. Uninjected wild type embryos showed a similar morphology (data not shown).

Unlike wild types, rescued *gpc4*$^{-/-}$ larvae showed no symplectic ossification; the larval element remained as a short, thick rod of cartilage attached to the more dorsal palatoquadrate (Fig. 5B). In some larvae, a separate symplectic was no longer visible, having fused with the palatoquadrate itself (Fig. 5D). In other larvae, the symplectic and palatoquadrate were still distinct, but connected by one or more cartilaginous bridges (Fig. 5E). We infer that the symplectic bone is routinely lost in *gpc4*$^{-/-}$ adults by failure of the embryonic chondrocytes to extend and ossify, followed by the incorporation of these remnant chondrocytes into the larval palatoquadrate. Interestingly, the hyomandibular cartilage of *gpc4*$^{-/-}$ larvae (Fig. 1) ossifies normally (Fig. 5A, B), maintaining an important linkage between the skull and jaw.

Loss of *gpc4* function leads to abnormal organization of adult craniofacial cartilages

In contrast to tetrapods, in fishes the skull is highly dynamic, with many adult bones remaining joined by flexible bands of connective tissue. Having observed abnormal chondrocyte arrangements in *gpc4*$^{-/-}$ larvae (Fig. 1I–K) and adults (Fig. 5C–F), we were interested in examining these areas in greater detail. In adults, we focused on the thin

cartilage band connecting the quadrate, metapterygoid, entopterygoid and palatine bone (Fig. 4A, B; asterisk). This tissue is derived from the larval palatoquadrate cartilage and its pterygoid process (Schilling and Kimmel, 1997). In *gpc4*$^{-/-}$ adults this cartilage band was particularly prominent, appearing broader than normal and filled with intensely blue-staining cells (Fig. 4C–F).

Microscopic examination of this adult cartilage revealed characteristic differences between wild types and mutants. In wild types (Fig. 6A), we observed an overlap between thin, Alizarin Red-stained bone and a single layer of rounded, Alcian Blue-positive chondrocytes, forming a faint purplish band (Fig. 6A1). The next region of cartilage contained highly elongated chondrocytes aligned parallel to the bone edge (Fig. 6A2). Finally, the central part of the cartilage contained chondrocytes that were larger, rounded and more randomly arranged (Fig. 6A3). In contrast, *gpc4*$^{-/-}$ mutant cartilage cells failed to form an overlapping connection with adjacent bones (Fig. 6B). Instead of a purple-stained border, a dense wall of strongly red-staining bone material bluntly abutted the blue cartilage band (Fig. 6B1). Most strikingly, in the adjacent layer the *gpc4*$^{-/-}$ chondrocytes were not elongated parallel to the bone margin but were round and disorganized (Fig. 6B2). The central part of the cartilage, although narrower, appeared similar to the wild type organization (Fig. 6B3).

The zebrafish palatoquadrate cartilage contains arcs of highly elongated chondrocytes, which fail to form in *gpc4*$^{-/-}$ embryos

The abnormal chondrocyte organization in the palatoquadrate cartilage of *gpc4*$^{-/-}$ adults prompted us to investigate further when these mutant defects arise. We were particularly interested in how chondrocytes arrange to form highly polarized arcs of cells oriented along the borders of perichondrial and endochondral ossifications. Examination of a series of wild type larvae revealed that the three zones of cartilage organization observed in the adult are in fact established early, within the first few weeks of larval life (~8 mm SL; Fig 6E). In contrast, chondrocytes of rescued *gpc4*$^{-/-}$ larvae at the same stage were not elongated parallel to the developing bone (Fig. 6F). Despite improper cell orientation, the cartilage cells in this area still stained strongly with Alcian Blue, suggesting normal chondrocyte differentiation.

To document in greater detail the dynamics of chondrogenesis and osteogenesis in the zebrafish palatoquadrate, we collected a developmental series of approximately 25 wild type fish (4–16 mm SL; Fig. 7). This series was intended to capture the interval from complete chondrification through endochondral ossification (Cubbage and Mabee, 1996). For clarity, only four representative stages (6, 10, 12 and 16 mm SL) are shown.

At the earliest larval stages examined (4 mm SL), the zebrafish palatoquadrate shows no signs of chondrocyte polarization; all of the cells are rounded and similar in shape (see Fig. 1A in (Nissen et al., 2006). In slightly older larvae, however (~6 mm SL), we observed two arcs of elongated chondrocytes, one anterior and one posterior (Fig. 7A, B). Both arcs were approximately 4–6 cells wide. The anterior arc extended from the base of the pterygoid process to the ventral margin of the palatoquadrate, just anterior to the tip of the symplectic. The posterior arc, initially less prominent, crossed the palatoquadrate near the midpoint of the symplectic. At this stage, early ossification of the endochondral and membranous bones had also begun (Fig. 7C, D).

By ~10 mm SL, both arcs of chondrocytes were more pronounced, and the cells in these zones were more elongated (Fig. 7E, F). Although by this stage the zebrafish had nearly doubled in body size and the entire cartilage element had grown significantly, the arcs were still narrow (4–6 cells wide) and their relative positions were not dramatically changed. Although the entire palatoquadrate still stained strongly with Alcian Blue, indicating a

cartilaginous matrix, Alizarin Red staining showed thin, fan-shaped perichondrial bones extending over the cartilage sheet. Confocal imaging of this area confirmed two sheets of bone, one medial and one lateral, surrounding the cartilage template (Supplementary Figure S2). The leading edges of this perichondrial ossification correspond closely to the underlying arcs of elongated chondrocytes.

In the oldest specimens analyzed (12–16 mm SL; Fig 7I–P), the growth of superficial perichondrial bone was followed by endochondral ossification of the quadrate and metapterygoid, as indicated by a loss of Alcian Blue staining. The regions of bony replacement extended towards, and eventually terminated at, the arcs of elongated chondrocytes initially established in the larva. At this point, chondrogenesis and osteogenesis in the palatoquadrate was essentially complete, leaving a persistent band of adult cartilage with a normal cellular arrangement (*e.g.*, Fig. 4) between adjacent endochondral bones.

Discussion

Although the basic principles of cartilage and bone formation are well established, the molecular mechanisms of skeletal morphogenesis are still not fully understood. To date, the zebrafish model is relatively underutilized in this respect, as much more is known about skeletal patterning in the larva than morphogenesis at later stages. In this investigation, we sought to extend what was known about alleles of *glypican 4* (*knypek)*, an extracellular mediator of signal transduction. We knew that *gpc4* mutations affected embryonic cell migration and polarization, leading to death at early larval stages; however, effects past this critical period were unknown. By rescuing *gpc4*$^{-/-}$ embryos with mRNA injections and rearing a small number of these for more than one year, we were able to study the effects of Glypican 4 deficiency on the craniofacial organization of juveniles and adults.

Gpc4 contributes to the morphogenesis of larval head cartilages and the adult skull

In rescued *gpc4*$^{-/-}$ embryos, craniofacial cartilages remained shortened and contained disorganized, rounded chondrocytes. This defect was greatest in the rod-shaped cartilage elements formed by chondrocyte flattening and cell-cell intercalation, including the ceratohyal, ethmoid, and symplectic. More posterior endochondral elements, such as the larval hyoid and parachordal plate, were less affected. These larval craniofacial abnormalities persisted into later stages. Despite achieving body sizes comparable to wild types, *gpc4*$^{-/-}$ adults had consistently smaller neurocrania with reduced anterior skulls. Although measured from a small sample of individuals, the morphometric features of mutant and wild type skulls were statistically robust, reflecting highly significant differences. We conclude that the lack of Glypican 4 activity in larval zebrafish causes a variable but repeatable phenotype of adult craniofacial anomalies. The persistence of these defects in adult teleosts, which grow slowly but continuously throughout life, also suggests that an early Glypican 4 deficiency cannot be entirely compensated for by later ossification or bone remodeling.

Abnormal chondrocyte stacking in *gpc4*$^{-/-}$ larvae interferes with normal symplectic ossification, altering the jaw suspension

The loss of the symplectic in adult *gpc4*$^{-/-}$ adults adds *glypican 4* to the list of genes that can change the number and arrangement of adult bones. Other examples include *Pitx1*, a transcription factor that modifies pelvic bones and body armor in sticklebacks (Bell et al., 2007) and endothelin1 (*Edn1*), a secreted peptide that alters pharyngeal cartilages (Kimmel, 2003; Kimmel et al., 2007). Unilateral or bilateral loss of the symplectic bone was highly penetrant, affecting 83% (10/12) of mutant adults. In these animals, a remnant of the

symplectic cartilage was fused with the adjacent palatoquadrate cartilage, and the nearby metapterygoid bone was expanded to link the quadrate and the hyomandibular. Difficulties in this remodeling may explain the small number of *gpc4*$^{-/-}$ larvae that survived to adulthood. No other cranial bones in *gpc4* mutant adults were absent, indicating that Glypican 4 is not essential for their formation or arrangement.

The teleost jaw has been studied extensively both as an anatomical innovation within vertebrates and as a system of biomechanical linkages adapted to diverse species' ecologies (Richard and Wainwright, 1995; Hernandez, 2000; Alfaro et al., 2004; Westneat et al., 2005). Specifically, the appearance of a symplectic is considered to be an innovation of neopterygians, first appearing in basal taxa such as bowfin (*Amia*) and gars (*Lepisosteus* sp.). Biomechanically, the symplectic forms an additional link between the quadrate and the hyoid, allowing greater jaw flexibility. In extant fishes symplectic morphology is highly variable, and the element can be reduced, fused to surrounding bones, or lost. Within Ostariophysi, the clade to which zebrafish belong, a prominent symplectic is found in Gonorynchiforms (Kohno et al., 1996), most Cypriniformes *(e.g., Danio, Cyprinus)* and Gymnotiformes (electric eels and knifefishes; *e.g., Eigenmannia*). However the large sister clade of Siluriformes (catfishes) and all tetrapods lack this element entirely (Gregory, 1933). Understanding the developmental plasticity of the jaw is thus interesting from an evolutionary perspective, as its components have undergone significant transformations among major vertebrate taxa.

Abnormal chondrocyte elongation in the larval palatoquadrate persists in the cranial cartilages of *gpc4*$^{-/-}$ adults

Unlike birds or mammals, adult teleosts have a kinetic skull in which some bones remain permanently connected with cartilage bands. In *gpc4*$^{-/-}$ adults we observed that the cranial cartilage deriving from the larval palatoquadrate was abnormal, indicating that the primary defect of larval cartilage morphogenesis was to some extent retained. To better compare the cartilage phenotypes of mutants and wild types, we closely examined the post-larval development and ossification of the palatoquadrate cartilage, as very limited information on its cellular architecture was available. After the initial cartilage template forms, two narrow arcs of elongated chondrocytes, one anterior and one posterior, appear within the structure. Fan-shaped areas of perichondrial bone are deposited on the medial and lateral sides of the template, and the leading edges of these sheaths parallel the arcs of elongated chondrocytes. When endochondral ossification occurs, mineralization also proceeds up to, but not past, the same boundary. Finally, the mature palatoquadrate cartilage can be divided into three areas: 1) far lateral regions where cartilage and bone cells overlap, 2) the near lateral arcs of highly polarized cartilage cells and 3) a medial region of rounded cartilage cells.

Abnormalities of palatoquadrate organization were first observed in *gpc4*$^{-/-}$ mutants around 6–8 mm SL (Fig. 6F). Instead of forming two well-defined arcs of elongated chondrocytes, disorganized, rounded chondrocytes were observed adjacent to the ossifying quadrate and metapterygoid bones. These defects persisted into *gpc4*$^{-/-}$ adults. The far lateral region was missing; in its place, abnormally thick bone was formed. In the near lateral region, the chondrocytes were rounded and disorganized instead of being narrowed and oriented parallel to the bony edge. This phenotype suggests that Gpc4, in addition to its influence on cartilage elongation and stacking in rod-shaped elements, also influences cell shape within a flat cartilage sheet.

The sequence of ossification we have observed in the zebrafish palatoquadrate cartilage is intriguingly similar to endochondral bone formation in other vertebrates. After a cartilage template is formed, the next step is superficial mineralization of perichondrial tissue, followed by cartilage replacement (Kronenberg, 2007). Classic endochondral ossification,

however, includes more dramatic changes in chondrocyte appearance, including greatly enlarged hypertrophic chondrocytes and apoptotic cartilage cells. In the zebrafish palatoquadrate we observed only minimal enlargement of chondrocytes before gradual loss of Alcian blue staining and replacement with bone. It remains to be seen what molecular markers of the classic vertebrate growth plate are expressed in this element. In general, the zebrafish palatoquadrate and its surrounding suite of endochondral and intramembraneous bones offer an interesting model to study how adjacent skeletal elements develop in a linked biomechanical system. This small, flat and relatively thin cartilage also has excellent optical properties, which should allow application of many of the cellular and molecular methods already developed for zebrafish embryos.

Molecular mechanisms of cranial cartilage patterning and morphogenesis

Numerous zebrafish mutations have been isolated that cause loss or reduction of cartilages in the second pharyngeal arch. The second arch comprises the hyoid, symplectic and ceratohyal in a dorsal-ventral series. Some mutations affect the entire arch due to altered expression of segment-specific *Hox* genes. If *hoxa2b* and *hoxb2a* are suppressed, the second arch converts to a jaw-like first arch (Hunter and Prince, 2002; Crump et al., 2006). Other mutations affect only a subset of second arch cartilages. Reductions in the ceratohyal and symplectic can be caused by mutations in *phospholipase C beta-3* (Walker, et al., 2007), *furin a* (Walker et al., 2006), *endothelin 1* (Miller et al., 2000) or *hand2* (Piotrowski et al., 1996; Yelon et al., 2000; Miller et al., 2003). Conversely, reductions in the hyomandibular occur in mutants lacking the transcription factor *foxi1* (Nissen et al., 2003). These observations have led to a morphogen gradient model for second arch skeletal patterning (Kimmel et al., 2007). Chondrocytes located where dorsalizing signals are high and ventral fates are suppressed become the hyoid and symplectic, while chondrocytes located ventrally receive a converse set of signals, forming the ceratohyal. Intermediate levels of dorsalizing and ventralizing signals are thought to pattern the hyo-symplectic jaw joint (Miller et al., 2003).

In contrast to mutants in which the dorsalmost or ventralmost second arch elements are the most severely affected, the primary defect of Glypican 4 deficiency is a loss of the intermediate element (the symplectic) followed by some reduction of the ventral element (the ceratohyal). Thus the primary defect of Glypican 4 deficiency does not appear to be second arch identity or patterning but the morphogenesis of particular cartilage elements within the arches, specifically those that require cartilage stacking to form elongated rods. Indeed, the *gpc4*$^{-/-}$phenotype extends well beyond the second arch to the cartilaginous palatoquadrate and neurocranium, as previously described. We infer from this that Glypican 4 globally controls cell elongation during cartilage morphogenesis in a manner analogous to its role during convergence and extension during gastrulation.

The *gpc4*$^{-/-}$ *(kny)* larval phenotype is similar to those described for *dackel* (*dak*) and *pinscher* (*pic*), two other zebrafish mutations affecting the biosynthesis of heparan sulfate proteoglycans (Clément, 2008). At 6 dpf, *dak* and *pic* mutant larvae have craniofacial cartilages that are shortened and full of rounded cells, similar to elements in *kny* larvae. However *dak* and *pic* mutants additionally show a global loss of markers associated with chondrocyte hypertrophy (*collagen 10a1*) and bone formation (*osterix*, *crossveinless*). Robust formation of endochondral and dermal bones in *kny* mutants, however, shows that Glypican 4 is not essential for these processes. We would, however, predict a local downregulation of ossification markers in the region of the symplectic, as this adult bone so frequently fails to form. Together, *gpc4*(*kny)*, *dak* and *pic* all support a role for heparan sulfate proteoglycans in cartilage morphogenesis. In contrast to *kny*, which encodes the zebrafish Glypican 4 core protein, the products of *dak* (a glycosyltranferase that catalyzes the production of heparan sulfates) and *pic* (a sulphate transporter responsible for sulfating

glycans) encode enzymes required for all cellular HSPGs. Thus the *knypek* mutant analyzed here identifies Glypican 4 as a specific mediator of cell signaling that regulates cartilage behavior during zebrafish skeletogenesis.

Because glypicans can bind multiple ligands, disruption of glypican function can affect one or more signaling pathways. Classically, Glypican 4 is part of the noncanonical Wnt/PCP pathway, controlling cellular migration during gastrulation and larval cartilage morphogenesis (Topczewski et al., 2001). Mutations in *wnt5b* gene cause cartilage defects similar to *gpc4*$^{-/-}$(Piotrowski et al., 1996; Rauch et al., 1997; Topczewski manuscript in preparation), suggesting that Glypican 4 acts as a co-receptor for this ligand. In mouse and chick, Wnt5a and Wnt5b are expressed in distinct domains of developing bones (Hartmann and Tabin, 2000; Church et al., 2002) and gain- and loss-of-function experiments indicate that these ligands regulate ossification by antagonistically controlling progenitor cell proliferation and differentiation (Yamaguchi et al., 1999; Yang et al., 2003). However, the fact that *gpc4*$^{-/-}$ adults have normal cartilage differentiation and, with the exception of the symplectic, normal bone formation, suggests that these processes are Glypican 4 independent. Because the role of Wnt5 ligands in regulating cartilage differentiation has not been established in zebrafish, however, we cannot exclude the possibility that these ligands may act differently in tetrapods and teleosts.

Although disruption of Wnt/PCP signaling is one potential consequence of loss of *glypican 4*, other pathways may also be affected. Recently, zebrafish Glypican 4 has been shown to regulate distribution of the canonical Wnt/beta-catenin antagonist Dkk1 (Hartmann and Tabin, 2000; Caneparo et al., 2007). Glypicans may also interact with other ligands involved in cartilage differentiation, particularly Hedgehogs (Capurro et al., 2008). Indian hedgehog is a master regulator of bone development, coordinating chondrocyte proliferation, chondrocyte differentiation and osteoblast differentiation (Kronenberg and Chung, 2001). Although Glypican 4 is not critical for Hedgehog signaling during early stages of development (Topczewski et al., 2001), we cannot rule out its involvement later in ontogeny.

In this study we have described several phenotypic changes associated with loss of Gpc4 function in zebrafish craniofacial development. By studying the adult phenotypes of *gpc4*$^{-/-}$mutants, we have identify an ongoing requirement for glypicans in the regulation of cartilage morphogenesis and maturation. It remains to be determined whether these phenotypes depend on the well-characterized role of Gpc4 as a part of the Wnt/PCP signaling pathway, or whether Gpc4 regulates other ligands during later stages of zebrafish ontogeny. In addition, we describe the normal chondrogenesis and osteogenesis of the zebrafish palatoquadrate cartilage, a useful system for further observations on cartilage and bone development within the jaw linkage. Future study of the palatoquadrate and its surrounding skeletal elements should further clarify the genetic and biomechanical factors controlling jaw anatomy, diversity, and function.

Experimental Procedures

Zebrafish strains, rearing, and rescue experiments

To study glypican signaling in post-larval zebrafish we used two *knypek* alleles, *kny*^{fr6} (ZDB-GENO-011120-2) and *kny*^{m818} (ZDB-GENO-011120-5) (Topczewski et al., 2001). All zebrafish were raised according to protocols approved by the IACUC of Children's Memorial Research Center, Chicago, IL. Rescue experiments injecting wild type *gpc4* mRNA (ZDB-GENE-011119-1) into embryos at the 1–2 cell stage were performed as described (Topczewski et al., 2001). This procedure rescues both *kny*^{fr6} and *kny*^{m818} homozygotes with high efficiency (> 90%); however, only 5–10% of the rescued mutant

embryos were viable past 7–10 dpf, and we were able to raise only the *kny*^{m818} individuals to adulthood. For our analysis of adult fish we used 12 *kny*^{m818} rescued fish that had survived more than one year (~2–3 cm standard length). These were compared to the same number of unrelated wild type zebrafish raised to approximately the same size and age. To follow the craniofacial development of mutant larvae in greater detail, we additionally collected intermediate stages of rescued *kny*^{fr6} and *kny*^{m818} homozygotes and their normal siblings at irregular intervals between 6 and 10 mm standard length (approximately 2–6 weeks of development at 28°C). Finally, to detect any haploinsufficiency or late ontogenetic effects of the amorphic allele of *kny*^{fr6}, nine adult heterozygotes were compared to their homozygous wild type siblings (*kny*$^{+/+}$); after detailed skeletal staining, no differences were observed (data not shown).

Whole-mount bone and cartilage staining

Adult fish were euthanized on ice and fixed in 4% paraformaldehyde/phosphate-buffered saline (PF/PBS, pH 7.6) for 1–2 days. After rinsing in PBS, they were transferred directly to 70% ethanol for long-term storage at room temperature. All specimens were photographed and measured for standard length (+/− 0.5 mm) in ethanol before further processing. Whole-mount stains for bone and cartilage were carried out according to (Taylor and Vandyke, 1985), with minor modifications to effectively clear larger specimens. After dehydration to 100% ethanol, adult fish were opened ventrally with fine scissors and gutted with forceps under a dissecting microscope. The eyes were removed and the bodies were completely skinned and descaled. To remove body fat, skinned specimens were soaked overnight in 100% acetone, then transferred immediately to Alcian Blue to begin the staining protocol. The enzymatic digestion step was accelerated by overnight incubation at 32–35°C (~18 hours). Stained specimens were stored in 85% glycerol/deionized water with 0.01% sodium azide as a preservative. To avoid fading, specimens were kept in the dark when not in use. For larval skeletal staining, we avoided loss of bone during the acidic cartilage-staining step by employing bone-only or cartilage-only protocols as described (Taylor and Vandyke, 1985), or, alternatively, a one-step neutral staining method to simultaneously label cartilage and bone (Walker and Kimmel, 2007).

Photography and microdissection

Whole, stained fish were photographed under a dissecting microscope to record original body proportions and staining intensity. The skeletons were then dissected to examine all of the craniofacial elements and obtain standard photographic views for morphometric analysis. Our dissections were organized to minimize the number of cuts and keep large groups of facial bones mutually attached. To avoid misclassification, all of the manipulations were carried out in the original labeled specimen dish. The skull and body were detached by cutting between the occiput and the first Weberian vertebra, and the skull was positioned ventral side up. Next, the paired pectoral fins were removed, and the branchial basket was isolated *in toto* from the ventral side. With the ventral neurocranium still facing up, a blunt probe was used to gently scrape all of the lateral facial bones away from any skull attachments. Finally, a microscalpel was used to separate the still-connected facial bones into left and right halves by cutting anteriorly between the paired maxillary and premaxillary bones. Both halves of the face were gently flattened under a small square of glass cut from a microscope slide, then photographed in the dissection dish with a millimeter micrometer. The isolated neurocranium was photographed ventrally and laterally, maintaining a consistent orientation and focus plane for each view.

Morphometric analysis

To compare the skeletal features of mutant and wild type neurocrania, two-dimensional configurations of landmark coordinates ($X_1Y_1…X_nY_n$) were acquired using tpsDIG2 (F.

James Rohlf; http://life.bio.sunysb.edu/morph/) and analyzed using the IMP suite of software programs (H. David Sheets; http://life.bio.sunysb.edu/morph/). Anatomical descriptions of the landmark points are shown in Figure 3; their anatomical descriptions are given in Table S1 (Supplementary Material). The nomenclature for adult skeletal bones follows (Cubbage and Mabee, 1996).

To compare the sizes of the neurocrania, we used centroid size, a shape-independent measure of area (Dryden and Mardia, 1998). To compare neurocranial shapes, we performed a generalized least-squares (GLS) superimposition analysis of landmark configurations, considering both lateral and ventral views of skull anatomy. Because each configuration of landmarks is rescaled independent of initial size, this is also called a "Procrustes" analysis (Zelditch et al., 2004). The IMP software program TwoGroup takes two populations (*e.g.*, wild types vs. mutants), calculates a reference or "average" configuration for each, and returns the partial (D_p) and full (D_f) Procrustes distance between the two references; D_f quantifies the overall differences between the two samples in shape space. The statistical significance of D_f was assessed by Goodall's F-test, a ratio of the between-group to within-group variance in the datasets being compared. In geometric terms, if individual landmark configurations are much farther away from the between-group reference configuration than they are from the within-group reference configuration, then F will be large, indicating a significant difference in skull shape independent of size.

Confocal imaging

The palatoquadrate cartilage was dissected from a series of wild type embryos (4–16 mm standard length, SL) stained with Alizarin Red, flat mounted in 50% glycerol and observed with a 510 META Zeiss confocal microscope. A z-series of images was collected using both red fluorescent and DIC channels. An orthogonal reconstruction was obtained with the Zeiss LSM program.

Supplementary Material

Refer to Web version on PubMed Central for supplementary material.

Acknowledgments

Grant information

NIH/NIDCR DE016678 to J. Topczewski

This work was supported in part by an NIH grant to JT (DE016678) and a DePaul University Research Council grant to EEL. We thank Drs. L. Solnica-Krezel and T. Van Raay for providing the mutant used in the initial studies, DePaul undergraduates C. Schumacher and K. Schwalbach for laboratory assistance, and Dr. H. David Sheets for copies of IMP software. Dr. K. Shimada and three anonymous reviewers provided critical comments on the manuscript.

References

Albertson RC, Yelick PC. Morphogenesis of the jaw: development beyond the embryo. Methods Cell Biol. 2004; 76:437–454. [PubMed: 15602886]

Albertson RC, Yelick PC. Fgf8 haploinsufficiency results in distinct craniofacial defects in adult zebrafish. Dev Biol. 2007; 306:505–515. [PubMed: 17448458]

Alfaro ME, Bolnick DI, Wainwright PC. Evolutionary dynamics of complex biomechanical systems: an example using the four-bar mechanism. Evolution. 2004; 58:495–503. [PubMed: 15119434]

Amsterdam A, Hopkins N. Mutagenesis strategies in zebrafish for identifying genes involved in development and disease. Trends Genet. 2006; 22:473–478. [PubMed: 16844256]

Barolo S, Posakony JW. Three habits of highly effective signaling pathways: principles of transcriptional control by developmental cell signaling. Genes Dev. 2002; 16:1167–1181. [PubMed: 12023297]

Bell MA, Ellis KE, Sirotkin HI. Pelvic skeleton reduction and Pitx1 expression in threespine stickleback populations. Novartis Found Symp. 2007; 284:225–239. discussion 239–244. [PubMed: 17710856]

Caneparo L, Huang YL, Staudt N, Tada M, Ahrendt R, Kazanskaya O, Niehrs C, Houart C. Dickkopf-1 regulates gastrulation movements by coordinated modulation of Wnt/beta catenin and Wnt/PCP activities, through interaction with the Dally-like homolog Knypek. Genes Dev. 2007; 21:465–480. [PubMed: 17322405]

Cano-Gauci DF, Song HH, Yang H, McKerlie C, Choo B, Shi W, Pullano R, Piscione TD, Grisaru S, Soon S, Sedlackova L, Tanswell AK, Mak TW, Yeger H, Lockwood GA, Rosenblum ND, Filmus J. Glypican-3-deficient mice exhibit developmental overgrowth and some of the abnormalities typical of Simpson-Golabi-Behmel syndrome. J Cell Biol. 1999; 146:255–264. [PubMed: 10402475]

Capurro MI, Xu P, Shi W, Li F, Jia A, Filmus J. Glypican-3 inhibits Hedgehog signaling during development by competing with patched for Hedgehog binding. Dev Cell. 2008; 14:700–711. [PubMed: 18477453]

Chiao E, Fisher P, Crisponi L, Deiana M, Dragatsis I, Schlessinger D, Pilia G, Efstratiadis A. Overgrowth of a mouse model of the Simpson-Golabi-Behmel syndrome is independent of IGF signaling. Dev Biol. 2002; 243:185–206. [PubMed: 11846487]

Church V, Nohno T, Linker C, Marcelle C, Francis-West P. Wnt regulation of chondrocyte differentiation. J Cell Sci. 2002; 115:4809–4818. [PubMed: 12432069]

Clément A, Wiweger M, von der Hardt S, Rusch M, Selleck S, Chien C, Roehl H. Regulation of zebrafish skeletogenesis by ext2/dackel and papst1/pinscher. PLoS Genet. 2008; 4:e1000136. [PubMed: 18654627]

Crump JG, Swartz ME, Eberhart JK, Kimmel CB. Moz-dependent Hox expression controls segment-specific fate maps of skeletal precursors in the face. Development. 2006; 133:2661–9. [PubMed: 16774997]

Cubbage CC, Mabee PM. Development of the cranium and paired fins in the zebrafish Danio rerio (Ostariophysi, Cyprinidae). Journal of Morphology. 1996; 229:121–160.

Dryden, I.; Mardia, K. Statistical shape analysis. John Wiley and Sons; 1998. p. 376

Elizondo MR, Arduini BL, Paulsen J, MacDonald EL, Sabel JL, Henion PD, Cornell RA, Parichy DM. Defective skeletogenesis with kidney stone formation in dwarf zebrafish mutant for trpm7. Curr Biol. 2005; 15:667–671. [PubMed: 15823540]

Filmus J, Selleck SB. Glypicans: proteoglycans with a surprise. J Clin Invest. 2001; 108:497–501. [PubMed: 11518720]

Fisher S, Halpern ME. Patterning the zebrafish axial skeleton requires early chordin function. Nat Genet. 1999; 23:442–446. [PubMed: 10581032]

Fisher S, Jagadeeswaran P, Halpern ME. Radiographic analysis of zebrafish skeletal defects. Dev Biol. 2003; 264:64–76. [PubMed: 14623232]

Fransson LA. Glypicans. Int J Biochem Cell Biol. 2003; 35:125–129. [PubMed: 12479862]

Gavaia PJ, Simes DC, Ortiz-Delgado JB, Viegas CS, Pinto JP, Kelsh RN, Sarasquete MC, Cancela ML. Osteocalcin and matrix Gla protein in zebrafish (Danio rerio) and Senegal sole (Solea senegalensis): comparative gene and protein expression during larval development through adulthood. Gene Expr Patterns. 2006; 6:637–652. [PubMed: 16458082]

Geisler R, Rauch GJ, Geiger-Rudolph S, Albrecht A, van Bebber F, Berger A, Busch-Nentwich E, Dahm R, Dekens MP, Dooley C, Elli AF, Gehring I, Geiger H, Geisler M, Glaser S, Holley S, Huber M, Kerr A, Kirn A, Knirsch M, Konantz M, Kuchler AM, Maderspacher F, Neuhauss SC, Nicolson T, Ober EA, Praeg E, Ray R, Rentzsch B, Rick JM, Rief E, Schauerte HE, Schepp CP, Schonberger U, Schonthaler HB, Seiler C, Sidi S, Sollner C, Wehner A, Weiler C, Nusslein-Volhard C. Large-scale mapping of mutations affecting zebrafish development. BMC Genomics. 2007; 8:11. [PubMed: 17212827]

Gregory W. Fish skulls: a study of the evolution of natural mechanisms. Trans Amer Philos Soc. 1933:75–481.

Gumienny TL, MacNeil LT, Wang H, de Bono M, Wrana JL, Padgett RW. Glypican LON-2 is a conserved negative regulator of BMP-like signaling in Caenorhabditis elegans. Curr Biol. 2007; 17:159–164. [PubMed: 17240342]

Hartmann C, Tabin CJ. Dual roles of Wnt signaling during chondrogenesis in the chicken limb. Development. 2000; 127:3141–3159. [PubMed: 10862751]

Hernandez LP. Intraspecific scaling of feeding mechanics in an ontogenetic series of zebrafish, Danio rerio. J Exp Biol. 2000; 203:3033–3043. [PubMed: 10976040]

Hunter MP, Prince VE. Zebrafish hox paralogue group 2 genes function redundantly as selector genes to pattern the second pharyngeal arch. Dev Biol. 2002 Jul.15:367–89. [PubMed: 12086473]

Khare N, Baumgartner S. Dally-like protein, a new Drosophila glypican with expression overlapping with wingless. Mech Dev. 2000; 99:199–202. [PubMed: 11091094]

Kimmel CB, Walker MB, Miller CT. Morphing the hyomandibular skeleton in development and evolution. J Exp Zoolog B Mol Dev Evol. 2007; 308:609–624.

Kimmel CB, Ullmann B, Walker M, Miller CT, Crump JG. Endothelin 1-mediated regulation of pharyngeal bone development in zebrafish. Development. 2003 Apr; 130(7):1339–51. [PubMed: 12588850]

Kohno H, Ordonio-Aguilar R, Ohno A, Taki Y. Morphological aspects of feeding and improvement in feeding ability in early stage larvae of the milkfish, Chanos chanos. Ichthyological Research. 1996; 43:133–140.

Kronenberg H. The role of the perichondrium in fetal bone development. Ann N Y Acad Sci. 2007; 1116:59–64. [PubMed: 18083921]

Kronenberg H, Chung U. The parathyroid hormone-related protein and Indian hedgehog feedback loop in the growth plate. Novartis Found Symp. 2001; 232:144–152. discussion 152–147. [PubMed: 11277077]

Miller CT, Schilling TF, Lee K, Parker J, Kimmel CB. sucker encodes a zebrafish Endothelin-1 required for ventral pharyngeal arch development. Development. 2000; 127:3815–3828. [PubMed: 10934026]

Miller CT, Yelon D, Stainier DY, Kimmel CB. Two endothelin 1 effectors, hand2 and bapx1, pattern ventral pharyngeal cartilage and the jaw joint. Development. 2003; 130:1353–1365. [PubMed: 12588851]

Nakato H, Futch TA, Selleck SB. The division abnormally delayed (dally) gene: a putative integral membrane proteoglycan required for cell division patterning during postembryonic development of the nervous system in Drosophila. Development. 1995; 121:3687–3702. [PubMed: 8582281]

Neuhauss SC, Solnica-Krezel L, Schier AF, Zwartkruis F, Stemple DL, Malicki J, Abdelilah S, Stainier DY, Driever W. Mutations affecting craniofacial development in zebrafish. Development. 1996; 123:357–367. [PubMed: 9007255]

Nissen RM, Amsterdam A, Hopkins N. A zebrafish screen for craniofacial mutants identifies wdr68 as a highly conserved gene required for endothelin-1 expression. BMC Dev Biol. 2006; 6:28. [PubMed: 16759393]

Nissen RM, Yan J, Amsterdam A, Hopkins N, Burgess SM. Zebrafish foxi one modulates cellular responses to Fgf signaling required for the integrity of ear and jaw patterning. Development. 2003; 130:2543–2554. [PubMed: 12702667]

Paine-Saunders S, Viviano BL, Zupicich J, Skarnes WC, Saunders S. glypican-3 controls cellular responses to Bmp4 in limb patterning and skeletal development. Dev Biol. 2000; 225:179–187. [PubMed: 10964473]

Pilia G, Hughes-Benzie RM, MacKenzie A, Baybayan P, Chen EY, Huber R, Neri G, Cao A, Forabosco A, Schlessinger D. Mutations in GPC3, a glypican gene, cause the Simpson-Golabi-Behmel overgrowth syndrome. Nat Genet. 1996; 12:241–247. [PubMed: 8589713]

Piotrowski T, Schilling TF, Brand M, Jiang YJ, Heisenberg CP, Beuchle D, Grandel H, van Eeden FJ, Furutani-Seiki M, Granato M, Haffter P, Hammerschmidt M, Kane DA, Kelsh RN, Mullins MC, Odenthal J, Warga RM, Nusslein-Volhard C. Jaw and branchial arch mutants in zebrafish II: anterior arches and cartilage differentiation. Development. 1996; 123:345–356. [PubMed: 9007254]

Rauch G, Hammerschmidt M, Blader P, Schauerte H, Strähle U, Ingham P, McMahon A, Haffter P. Wnt5 is required for tail formation in the zebrafish embryo. Cold Spring Harb Symp Quant Biol. 1997; 62:227–234. [PubMed: 9598355]

Richard B, Wainwright P. Scaling the feeding mechanism of largemouth bass (Micropterus salmoides): kinematics of prey capture. J Exp Biol. 1995; 198:419–433. [PubMed: 9318056]

Schilling TF, Kimmel CB. Musculoskeletal patterning in the pharyngeal segments of the zebrafish embryo. Development. 1997; 124:2945–2960. [PubMed: 9247337]

Solnica-Krezel L, Stemple DL, Mountcastle-Shah E, Rangini Z, Neuhauss SC, Malicki J, Schier AF, Stainier DY, Zwartkruis F, Abdelilah S, Driever W. Mutations affecting cell fates and cellular rearrangements during gastrulation in zebrafish. Development. 1996; 123:67–80. [PubMed: 9007230]

Taylor WR, Vandyke GC. Revised procedures for staining and clearing small fishes and other vertebrates for bone and cartilage study. Cybium. 1985; 9:107–120.

Topczewski J, Sepich DS, Myers DC, Walker C, Amores A, Lele Z, Hammerschmidt M, Postlethwait J, Solnica-Krezel L. The zebrafish glypican knypek controls cell polarity during gastrulation movements of convergent extension. Dev Cell. 2001; 1:251–264. [PubMed: 11702784]

Viviano BL, Silverstein L, Pflederer C, Paine-Saunders S, Mills K, Saunders S. Altered hematopoiesis in glypican-3-deficient mice results in decreased osteoclast differentiation and a delay in endochondral ossification. Dev Biol. 2005; 282:152–162. [PubMed: 15936336]

Walker MB, Kimmel CB. A two-color acid-free cartilage and bone stain for zebrafish larvae. Biotech Histochem. 2007; 82:23–28. [PubMed: 17510811]

Walker MB, Miller CT, Coffin Talbot J, Stock DW, Kimmel CB. Zebrafish furin mutants reveal intricacies in regulating Endothelin1 signaling in craniofacial patterning. Dev Biol. 2006; 295:194–205. [PubMed: 16678149]

Walker MB, Miller CT, Swartz ME, Eberhart JK, Kimmel CB. phospholipase C, beta 3 is required for Endothelin1 regulation of pharyngeal arch patterning in zebrafish. Dev Biol. 2007 Apr 1; 304(1): 194–207. [PubMed: 17239364]

Westneat MW, Alfaro ME, Wainwright PC, Bellwood DR, Grubich JR, Fessler JL, Clements KD, Smith LL. Local phylogenetic divergence and global evolutionary convergence of skull function in reef fishes of the family Labridae. Proc Biol Sci. 2005; 272:993–1000. [PubMed: 16024356]

Witten PE, Hansen A, Hall BK. Features of mono- and multinucleated bone resorbing cells of the zebrafish Danio rerio and their contribution to skeletal development, remodeling, and growth. J Morphol. 2001; 250:197–207. [PubMed: 11746460]

Yamaguchi TP, Bradley A, McMahon AP, Jones S. A Wnt5a pathway underlies outgrowth of multiple structures in the vertebrate embryo. Development. 1999; 126:1211–1223. [PubMed: 10021340]

Yang Y, Topol L, Lee H, Wu J. Wnt5a and Wnt5b exhibit distinct activities in coordinating chondrocyte proliferation and differentiation. Development. 2003; 130:1003–1015. [PubMed: 12538525]

Yelon D, Ticho B, Halpern ME, Ruvinsky I, Ho RK, Silver LM, Stainier DY. The bHLH transcription factor hand2 plays parallel roles in zebrafish heart and pectoral fin development. Development. 2000; 127:2573–2582. [PubMed: 10821756]

Zelditch, M.; Swiderski, D.; Sheets, H.; Fink, W. Geometric morphometrics for biologists: a primer. London: Elsevier; 2004.

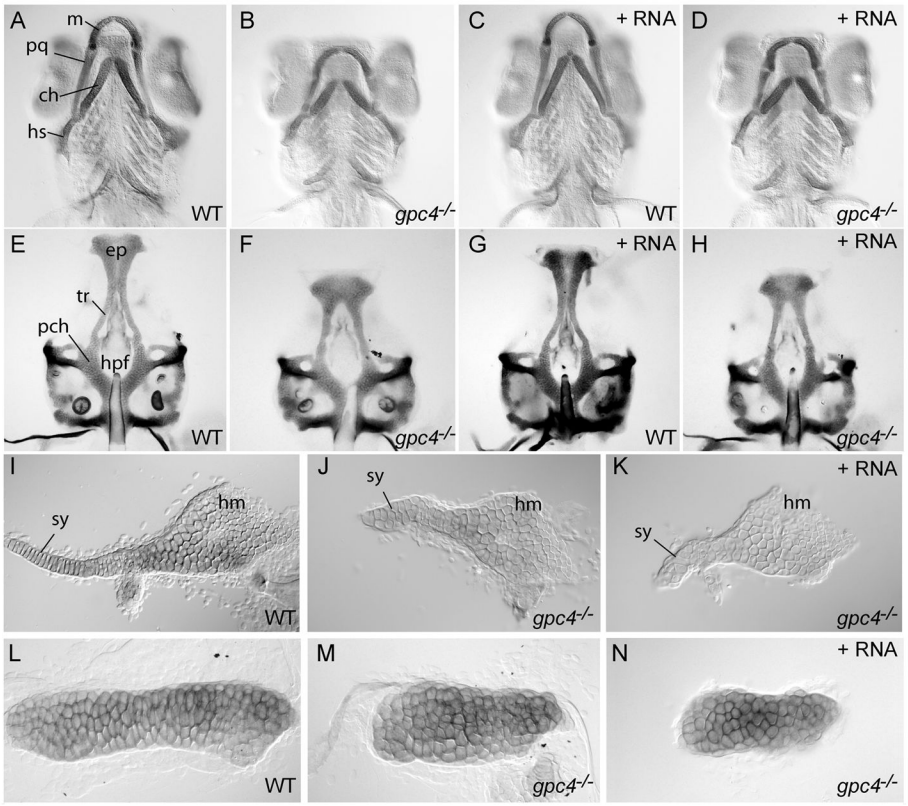

Figure 1. *gpc4* mRNA fails to rescue craniofacial cartilage morphology of *gpc4*$^{-/-}$ (*knypek*) embryos

A–D) Ventral view of zebrafish pharyngeal arch cartilages stained with Alcian Blue at 7 days post fertilization (dpf). Compared to wild-type siblings (A), the palatoquadrate, ceratohyal and symplectic cartilages of *gpc4*$^{-/-}$ larvae were shorter and thicker (B). Wild type siblings injected with synthetic *gpc4* mRNA developed normally (C). Injection of the same dose of synthetic mRNA fully rescued gastrulation defects of *gpc4*$^{-/-}$ embryos (Topczewski et al. 2001), but the mutant cartilage phenotype was not suppressed (D).

E–H) Ventral view of isolated larval neurocrania (7 dpf). Compared to wild types (E), the anterior ethmoid plate (ep) of *gpc4*$^{-/-}$ mutant larvae was shortened and the trabeculae (tr) were farther apart, causing an enlarged hypophyseal fenestra (hpf). The posterior parachordal plate (pch) was relatively normal. Wild type siblings injected with synthetic *gpc4* mRNA developed normal neurocrania (G), but in injected mutants the neurocranial defect was not suppressed (H).

I–K) Flat-mounted hyosymplectic cartilages (7dpf). Compared to wild types (I), *gpc4*$^{-/-}$ larvae showed a severely shortened symplectic region (sy, J). The hyomandibular region (hm) was less affected. This defect in *gpc4*$^{-/-}$ larvae was not suppressed by *gpc4* mRNA injection (K).

L–N) Flat-mounted ceratohyal cartilages (7 dpf). The ceratohyal of a wild type embryo (L) is much longer than that of a *gpc4*$^{-/-}$ embryo (M). The failure of ceratohyal cartilage elongation is not suppressed by injecting *gpc4* mRNA into a *gpc4*$^{-/-}$ embryo (N).

ch = ceratohyal; **ep** = ethmoid plate; **hpf** = hypopophyseal fenestra; **hs** = hyosymplectic; **m** = Meckel's cartilage; **pch** = parachordal plate; **pq** = palatoquadrate; **sy** = symplectic; **tr** = trabeculae.

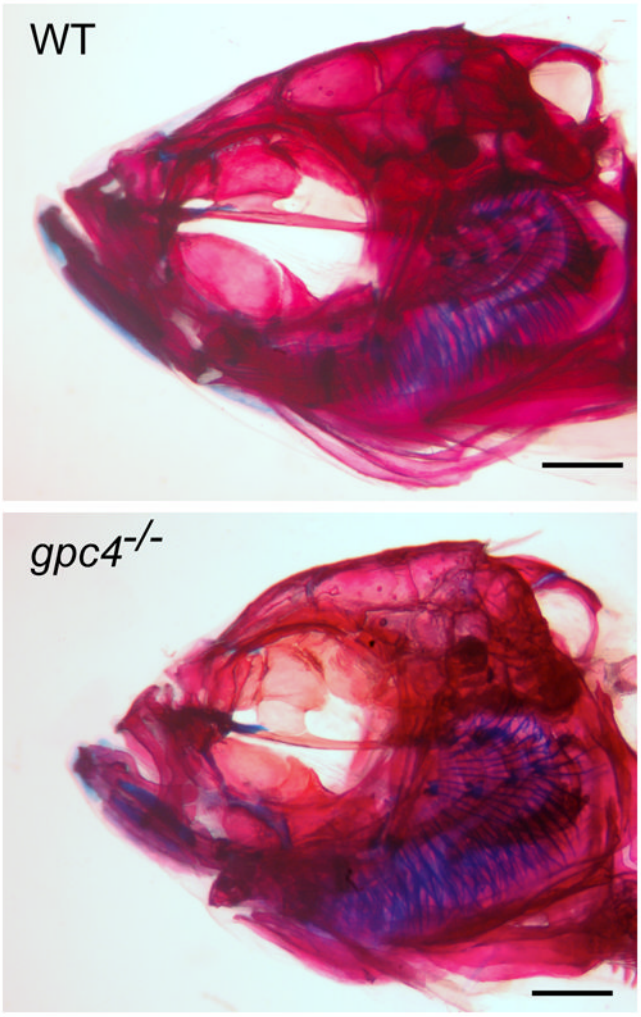

Figure 2. Cranial morphology of rescued *gpc4*$^{-/-}$ (*knypek)* mutants

Top: Wild type adult. Bottom: *gpc4*$^{-/-}$ mutant adult. Both fish are >1 yr of age and are photographed at the same scale (scale bar =1 mm). *gpc4*$^{-/-}$ fish are similar to comparable wild type fish in size and overall body proportions (data not shown) but have smaller heads, a domed skull, and shorter jawbones.

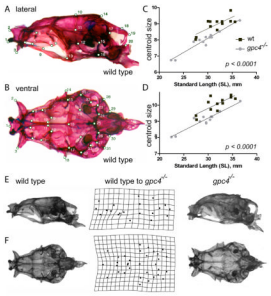

Figure 3. Size and shape comparison of wild type and *gpc4*$^{-/-}$ neurocrania

Locations of twenty lateral (A) and thirty-three ventral (B) skull landmarks used in the study. A complete description of each landmark is given in Table S1 (Supplementary Material). In both views, a wild type skull is shown. C, D) Linear regression of lateral (C) and ventral (D) skull centroid size vs. standard length for wild type (wt) and *gpc4*$^{-/-}$ mutant zebrafish. *gpc4*$^{-/-}$neurocrania are significantly smaller than wild type neurocrania across a wide range of body sizes, as indicated by the significant downward shift in the *gpc4*$^{-/-}$ regression line ($p < 0.0001$ for differences in intercept). E) Lateral and F) ventral views of a wild type (left column) and *gpc4*$^{-/-}$(right column) zebrafish skull. Center column: Deformation grid of neurocranial landmarks used in the study, derived from Procrustes superimposition of all wild type (n=12) and *gpc4*$^{-/-}$ (n=12) specimens. The grid indicates how the configuration of landmarks (A, B) must be altered to “convert” a wild type skull (left) into a mutant skull (right). Perfectly square cells indicate no difference in mean shape between mutants and wild types; deviations from squares indicate the regions of local shape difference between the two groups.

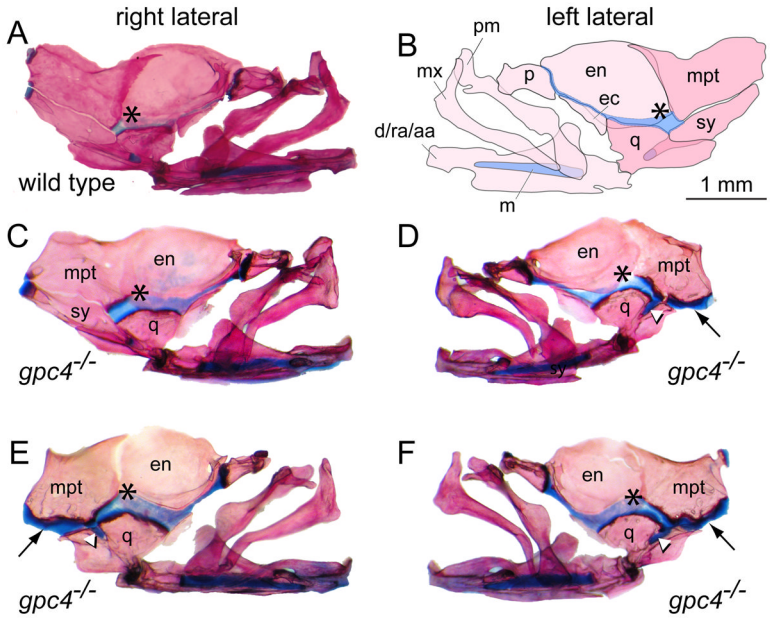

Figure 4. Loss of the symplectic bone in *gpc4*$^{-/-}$ mutant zebrafish

A) Right lateral facial bones of a wild type zebrafish, stained with Alcian Blue/Alizarin Red. Anterior is to the right. (*****) = palatoquadrate cartilage.

B) Mirror-image illustration of the facial bones and cartilages shown in (A). Anterior is to the left.

C, D) Unilateral loss of the symplectic in a *gpc4*$^{-/-}$ adult. The right side facial bones are normal (C); however, the left side of the same individual (D) lacks the symplectic (**sy**) ventral to the metapterygoid bone (**mpt**). In the absence of the symplectic, the metapterygoid and quadrate bones are attached by an ectopic band of cartilage (black arrow, D–F). A stub of cartilage fills the notch in the quadrate where the symplectic normally lies (white arrowhead, D–F). Note that relative to wild type (A), the palatoquadrate cartilage in *gpc4*$^{-/-}$ individuals appears broader and more deeply stained with Alcian Blue (asterisk, A–F).

E, F) Bilateral loss of the symplectic in a second *gpc4*$^{-/-}$ adult. The morphology of both sides is similar to D. **d/ra/aa**, dentary/retroarticular/angular; **ec**, ectopterygoid; **en**, entopterygoid; **m**, Meckel's cartilage; **mx**, maxilla; **mpt**, metapterygoid; **p**, palatine; **pm**, premaxilla; **q**, quadrate; **sy**, symplectic. All images are at the same magnification. Scale bar = 1 mm.

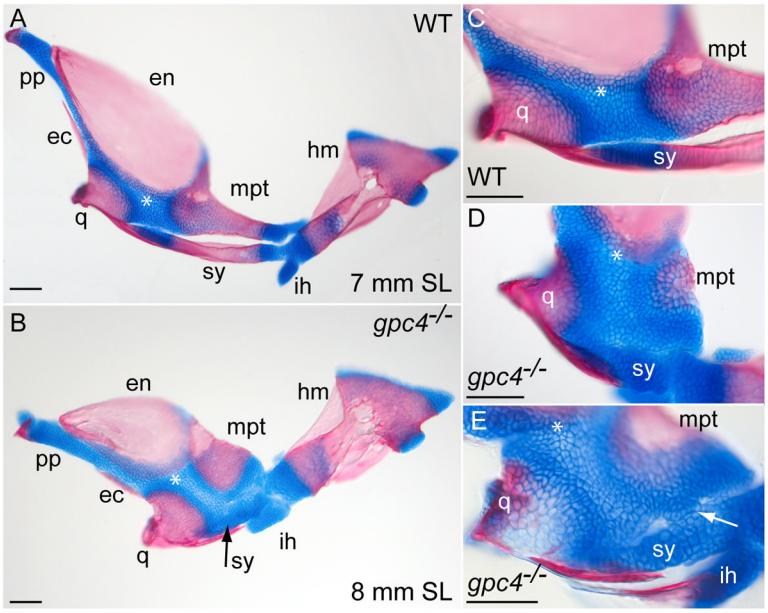

Figure 5. Intermediate stages of symplectic bone development in *gpc4*$^{-/-}$ larvae

A) Flat-mounted facial bones and cartilages from a 7-mm wild type larva (SL = standard length). Anterior is to the left. At this stage, the symplectic (**sy**) is a separate bone with two cartilaginous ends.

B) The corresponding region of an 8-mm *gpc4*$^{-/-}$ larva. The reduced symplectic cartilage (**sy**, black arrow) has not ossified and is fused to the adjacent palatoquadrate. All other ossification centers are present.

C) Magnification of the wild type embryo in (A).

D) Magnified palatoquadrate cartilage in a second *gpc4*$^{-/-}$ larva. The reduced symplectic (**sy**) is a ball of cartilage broadly connected with the palatoquadrate cartilage (*). E) Symplectic region of a third *gpc4*$^{-/-}$ larva. A cluster of chondrocytes (arrow) forms a bridge between the reduced symplectic and the palatoquadrate. The quadrate is only partially mineralized. Abbreviations are as in Fig. 1 and 5. **ih**, interhyal; **pp**, pterygoid process. Scale bar = 100 μm.

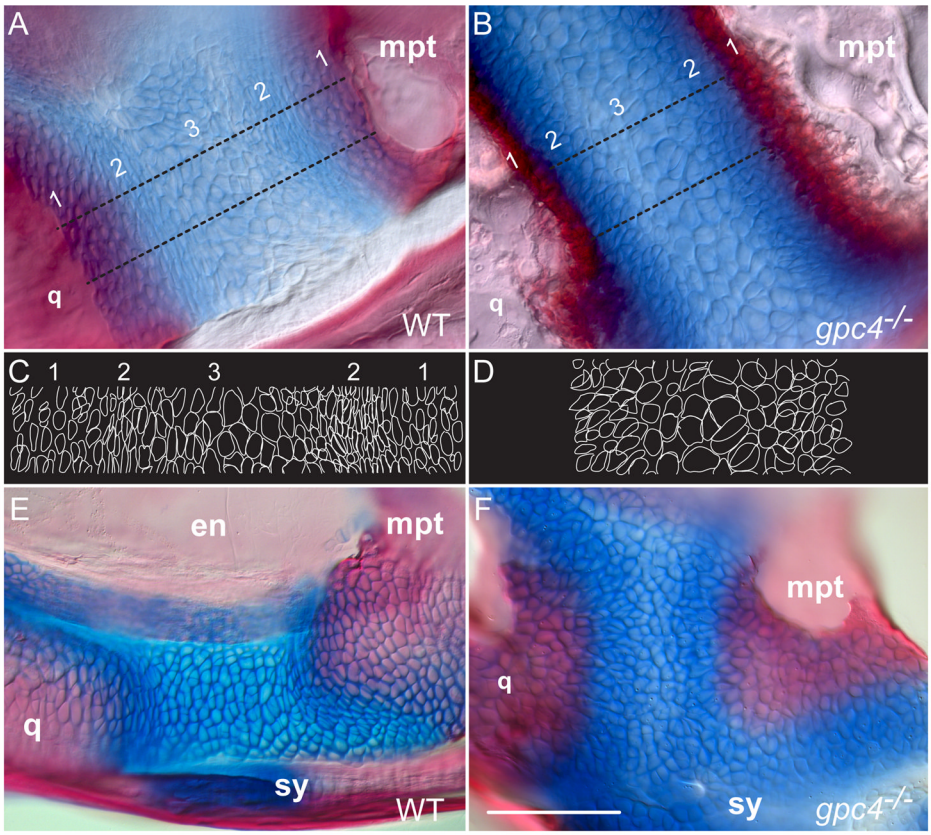

Figure 6. Adult *gpc4*$^{-/-}$ zebrafish lack elongated chondrocytes in the adult and juvenile palatoquadrate cartilage

A, B) Magnification of the adult cartilage band connecting the quadrate and metapterygoid bones. The wild type cartilage (A) has three regions: 1) bone overlapping with adjacent cartilage, 2) elongated chondrocytes parallel to the bone border and 3) a central region of larger, rounded chondrocytes. In *gpc4*$^{-/-}$ adults all three regions are modified (B). There is reduced overlap between bone and cartilage and a thickened bone border (region 1), no strongly elongated chondrocytes (region 2) and darker Alcian Blue staining overall (2 and 3).

C, D) Outlines of cells traced from the regions between the dotted lines in (A) and (B), respectively. Note the elongated cell boundaries in wild type region 2, which are absent in *gpc4*$^{-/-}$ mutants.

E, F) The adult defect of chondrocyte organization originates in the early larval palatoquadrate (~8 mm SL). The elongated cartilage cells present in wild type larvae (E) are rounded in *gpc4*$^{-/-}$ mutants (F). **en** = endopterygoid; **mpt** = metapterygoid; **q** = quadrate; **sy** = symplectic. Scale bar = 100 μm.

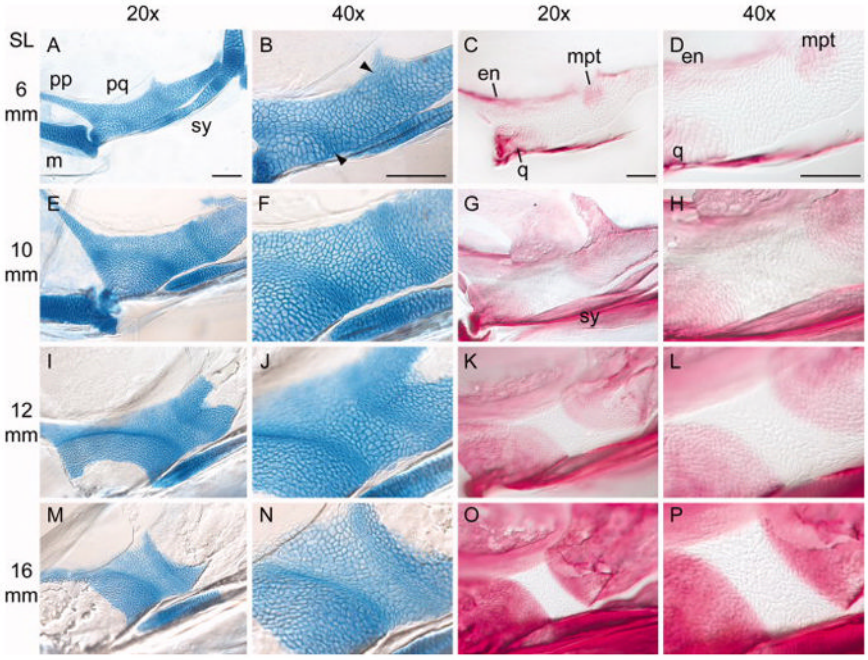

Figure 7. Developmental series of zebrafish palatoquadrate ossification

Flat-mounted views of larval zebrafish palatoquadrates. Anterior is to the left. For description, see text. SL = standard length of the fish (in mm). A–D) 6 mm SL, E–H) 10 mm SL; I–L) 12 mm SL; M–P) 16 mm SL. Stained specimens were cleared in 50% glycerol, flattened under a coverslip, and imaged with Nomarski optics. The images in the second and fourth columns (40x) are optical magnifications of the specimens in the first and third columns (20x). All images in a column are shown at the same magnification. Abbreviations are as in Fig. 5. Arrowheads point the arcs of elongated chondrocytes. All scale bars = 100 μm.

Table 1

Goodall's F-test for shape differences among groups

Specimens Compared	D_p [95%CI]	F	df	p
lateral skull, wt *vs.* *gpc4*$^{-/-}$	0.056 [0.052–0.071]	4.48	36, 576	<0.0000001
ventral skull, wt *vs.* *gpc4*$^{-/-}$	0.049 [0.046–0.059]	6.99	62, 1054	<0.0000001

D_p = partial Procrustes difference; df = degrees of freedom